

Development and evaluation of an AI System for early detection of Covid-19 pneumonia using X-ray (Student Consortium)

Mohit Mishra

*Electronics and Communication Dept.
IIT Guwahati, India
mohitmishra2022@gmail.com*

Varun Parashar

*Computer Science Dept.
IIT Guwahati, India
parasharvarun202@gmail.com*

Rushikesh Shimpi

*Computer Science Dept.
IIT Guwahati, India
rushikeshshimpi746@gmail.com*

Abstract—This paper aims to integrate AI (Artificial Intelligence) with medical science to develop a classification tool to recognize Covid-19 infection and other lung ailments. Four conditions evaluated were Covid-19 pneumonia, non-Covid-19 pneumonia, pneumonia and normal lungs. The proposed AI system is divided into 2 stages. Stage 1 classifies chest X-Ray volumes into pneumonia and non-pneumonia. Stage 2 gets input from stage 1 if X-ray belongs to pneumonic class and further classifies it into Covid-19 positive and Covid-19 negative.

Index Terms—Covid-19, coronavirus, Deep learning, chest X-ray, radiology images

I. INTRODUCTION

Deep learning having risen as the core technology of Artificial Intelligence (AI) has been found to significantly diagnose lung diseases with great accuracy [1, 2]. X-rays have been helpful to diagnose and screen patients for Covid-19 in initial stages [3].

In our work we aim to develop a classification framework to classify chest X-ray images of patients through 2 stages. Stage 1 classifies the X-rays into normal (healthy) and pneumonic patients and stage 2 further classifies the pneumonia affected patients into Covid-19 positive and Covid-19 negative based on Convolutional Neural Networks (CNN) [4]. Conditions evaluated includes normal lungs (healthy), pneumonia affected patients, Covid-19 positive and Covid-19 negative patients. The infected region usually includes the lower lobes. Distinct patterns like ground glass opacity, consolidation and thickened interlobular and interlobular septa [5, 6] can be analysed with deep learning methods. Furthermore, localisation of the lesions will enhance the quality of management and any deviation leading to complexities can be remotely observed. Common pathological detour is pleural effusion [7] which requires immediate pleural tapping thus limiting the dyspnea. Thus, this paper aims to save time and bring about an upgrade in our diagnostic capabilities.

II. METHODOLOGY

A. Image Acquisition

Total image dataset includes 1,878 X-ray images out of which 570 pneumonic and 630 non-pneumonic X-ray images

were procured from open image database from 2018 and 369 Covid-19 positive images were procured from open image database available at Società Italiana di Radiologia Medicae Interventistica (SIRM) and radiopaedia.org which included X-ray reports of patients aged 25-67 years old. Additionally, 309 Covid-19 negative X-ray images were also procured from the open database of European Society of Radiology (ESR).

B. Data Preprocessing

Appropriate preprocessing of the training data was done for eviction of heavily degraded images that would cost the accuracy of the trained model. The data was augmented which includes rotation (± 10 percent), left and right shift ($\pm 10\%$), height shift ($\pm 10\%$), zoom in (20%). The X-ray image was normalized by $1/225$. The training dataset obtained after data augmentation resulted in a total number of 15,024 X-ray images from a limited dataset.

III. PROPOSED ARCHITECTURE

The proposed 2D CNN architecture will be used to detect Covid-19 positive patients from the X-ray volumes as shown in Fig.1 and Fig.2. The overall architecture is divided into 3 parts namely entry flow, middle flow and exit flow. The entry flow facilitates as the initial part of the architecture which accepts the X-ray volumes, extracts the features and passes it on to the middle flow of the architecture.

Entry flow is constructed from three 2D convolutional layers with kernel size of 7×7 , 1×1 and 3×3 respectively, 2D max pooling layers with kernel size and stride each of 3×3 and 2 respectively, 2 batch normalization and 2 inception blocks. The input layer accepts $224 \times 224 \times 3$ sized X-ray volumes and returns $56 \times 56 \times 256$ features volume to the middle layer. Middle flow consists of 2 connected blocks, dense blocks and transition blocks where 'k' is the consecutive dense block connected to each other and 't' is consecutive transition block, where each connected layer is a combination of k^* dense block + t^* transition block with their respective values as in Table. 1.

Middle flow is overall constructed from 4 connected layers. Middle flow processes the output of entry flow of $56 \times 56 \times 256$

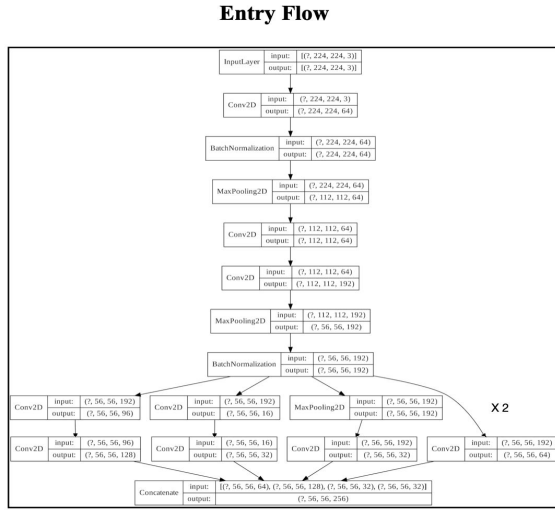


Fig. 1: The CovAI-Net Architecture - Entry Flow.

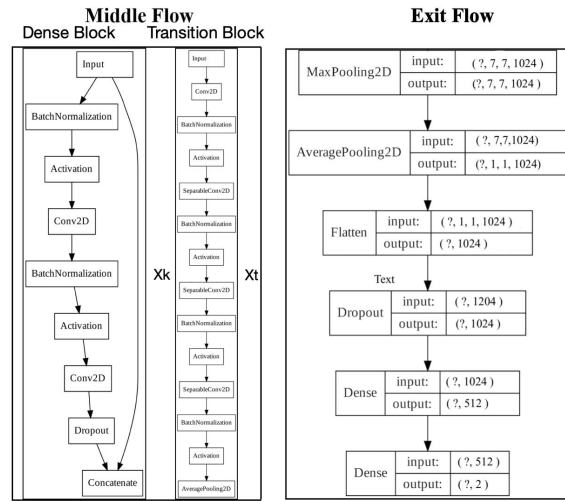


Fig. 2: The CovAI-Net Architecture - Middle Flow and Exit Flow.

size and returns $7 \times 7 \times 1024$ feature volumes to exit flow. The third part of the architecture is the exit flow. Exit flow facilitates the classification of feature volumes. It is a combination of 2D max pooling, 2D average pooling and fully connected layers. The kernel size and stride of 2D max pooling layers is $2 \times 2 \times 1$ respectively. 2D average pooling layer has a kernel size of 7×7 and stride 1.

Exit flow further classifies the feature volumes acquired by middle flow into required classes that are pneumonia affected, non-pneumonia affected/Covid-19 positive and Covid-19 negative.

Table. 1: Values of dense block and transition block in each connected layer.

Connected Layers #	Dense Block (k)	Transition Block (t)
1	6	3
2	16	3
3	28	3
4	28	0

IV. IMPLEMENTATION

We propose a 2D CNN named CovAI-Net which classifies potential Covid-19 patients using their chest X-ray image as shown in Fig. 3. The proposed CovAI-Net architecture predicts Covid-19 positive patients through 2 stages. The 1st stage includes classifying the X-ray image into 2 classes - pneumonia affected and normal cases.

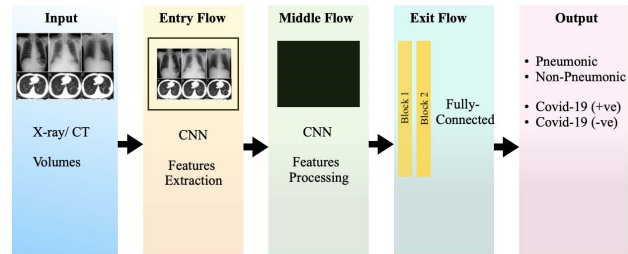


Fig. 3: Schematic diagram of the CovAI-Net Architecture.

If the X-ray image gets classified as pneumonic case, then the image will again go through the work flow discussed in Fig. 4 and will be classified into further two classes : Covid-19 affected and non-Covid-19 cases.

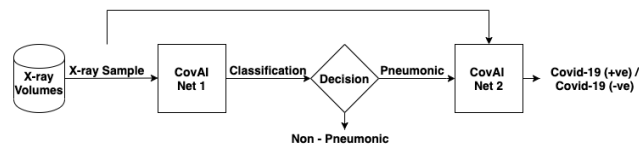


Fig. 4: Workflow of CovAI system.

The proposed architecture developed on keras [8] framework using Tensorflow backend is inspired by 3 state-of-the-art architectures - Inception [8], DenseNet [10], Xception [11], and are combined by selecting appropriate features from all, smooth gradient flow and fast convolution respectively. The model is implemented using 2D convolutions as it is easy to train it with more training samples which results in higher accuracy.

Hyperparamters used : optimizer = Adam [12], learning rate = 0.001, dropout rate = 0.3, loss = binary cross-entropy, kernel initializer = he uniform, batch size = 32, activations = ReLU[13], softmax[13].

V. EVALUATION AND RESULTS

A. Methodology

The following section summarizes training, validation and testing analysis. The CovAI-Net architecture is trained separately for both stage 1 and stage 2 to classify the input data into required classes. For stage 1 of classification, the architecture was trained on dataset of pneumonic and non-pneumonic X-rays. Further for stage 2, the architecture was trained on dataset of Covid-19 positive and Covid-19 negative X-rays to classify the pneumonic X-ray into Covid-19 positive and Covid-19 negative. This 2 stage training ensured better accuracy for predicting Covid-19 including pneumonia and increasing accuracy on the limited dataset.

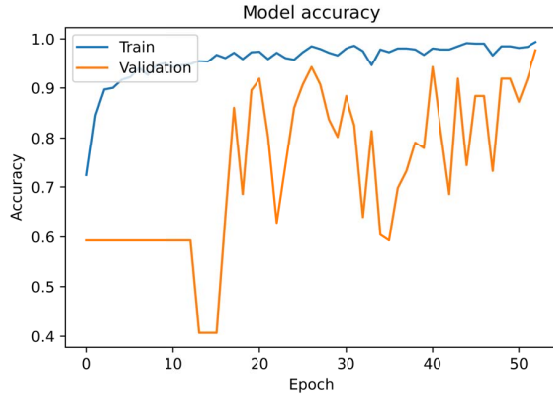


Fig. 5: Model Accuracy of Stage 1.

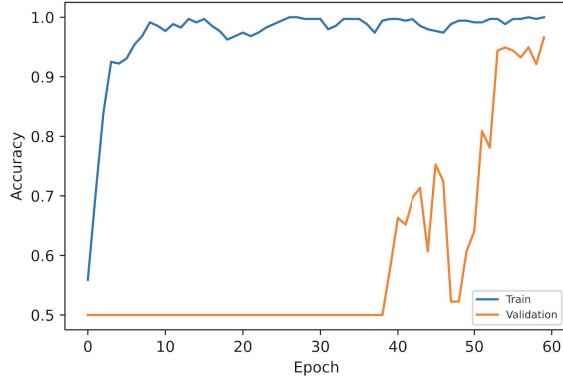


Fig. 6: Model Accuracy of Stage 2.

During the course of testing on X-ray volumes we achieved a maximum accuracy of 96.5% for stage 1 classification and 98.31% for stage 2 classification which can be validated from Fig. 5 and Fig. 6. Also the output of the CovAI-Net architecture can be advocated by the confusion matrix for stage 1 in Table. 2 and for stage 2 in Table. 3 respectively.

The CovAI-Net was trained on augmented dataset of 15024 X-ray images where each X-ray image was augmented using techniques mentioned in Section II.B. For training CovAI-Net

architecture techniques like multiprocessing, parallel programming and distributed computing were used. The architecture was trained on Nvidia Tesla K80 GPU.

Table. 2: Confusion matrix of stage 1

Predicted/Actual	Non-Pneumonic	Pneumonic
Non-Pneumonic	97	4
Pneumonic	3	96

Table. 3: Confusion matrix of stage 2

Predicted/Actual	Covid-19 Positive	Covid-19 Negative
Covid-19 Positive	89	0
Covid-19 Negative	3	86

B. Mathematical Analysis

To analyze the testing and confusion matrix of CovAI-Net architecture we used measures like precision, sensitivity, specificity, F1 score, PPV and NPV given as percentage in the classification report Table. 4 and Table. 5. During the entire testing procedure of test X-ray volume dataset we used the trained Cov-AI network to predict the probability of covid-19 positive, covid-19 negative pneumonic and non-pneumonic(normal lungs). All the 4 classes pneumonic, non-pneumonic, Covid-19 positive and Covid-19 negative were analyzed using the aforementioned measures to validate the proposed architecture.

Table. 4: Classification report I

Stages	Classes	Precision	Sensitivity	Specificity
1	Non-Pneumonic	96.04 %	97 %	96 %
	Pneumonic	96.97 %	96 %	97 %
2	Covid-19 +ve	100 %	96.74 %	100 %
	Covid-19 -ve	97.74 %	100 %	96.63 %

Table. 5: Classification report II

Stages	Classes	F1-Score	PPV	NPV
1	Non-Pneumonic	96.52 %	96.03 %	96.97 %
	Pneumonic	96.48 %	96.96 %	96.04 %
2	Covid-19 +ve	98.34 %	100 %	96.63 %
	Covid-19 -ve	98.34 %	96.62 %	100 %

The trained CovAI-Net model was tested on randomly collected data of 86 X-ray volumes. Our proposed system demonstrated a good real life prediction accuracy by predicting 84 true results and 2 false results. Some real life predictions by the model are demonstrated in Fig. 7.

The changes in sensitivity (True positive rate) and specificity (1-False positive rate) at different threshold can be observed from Fig. 8 and Fig. 9. We achieved an AUC score of 0.986 and 0.972 for stage 1 and 2 respectively.

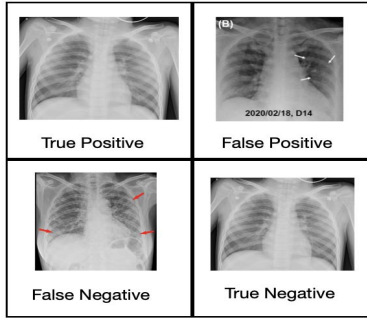


Fig. 7: Test outputs for covid-19 positive and covid-19 negative cases

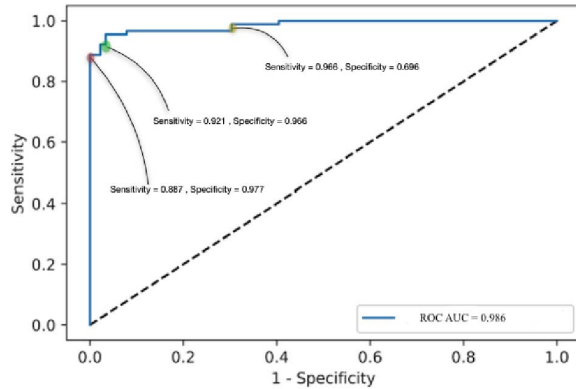


Fig. 8: ROC curve of Stage 1.

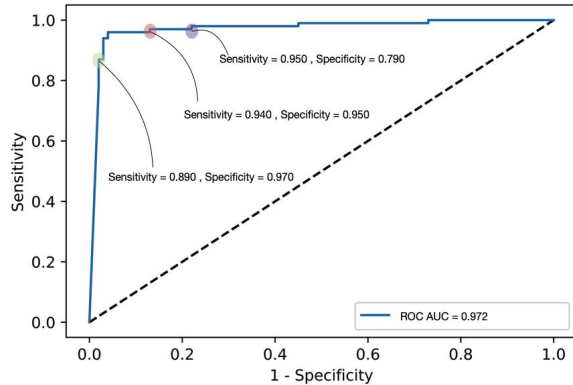


Fig. 9: ROC curve of Stage 2.

VI. DISCUSSION

The motivation of this work was to utilize artificial intelligence to solve the problem of shortage of interpretation of X-ray images in this fast spreading pandemic. This AI system would not only act as a tool for clinicians and radiologists but will also complement the rRT-PCR test and alleviate its shortcomings [14]. There were many studies which showed promising results for application of AI into

medical field [15, 16, 17] which acted as a catalyst for this study.

The development of CovAI-Net was a challenging task pertaining to availability of less radiological data of Covid-19 positive patients. This problem was addressed using the data augmentation techniques. Due to increased workload, radiologists were not available to label the lesions in X-ray volumes thus X-ray volumes were only labeled on the level of patients (i.e. Covid-19 positive and Covid-19 negative). The problem was solved by regarding the Covid-19 detection problem as a weakly supervised learning problems [18] i.e. detecting the potential Covid-19 positive X-ray without annotating the regions of Covid-19 lesions. The third challenge faced was feature extraction from hazy and cloudy X-ray volumes. This problem was resolved using Inception block of the Inception architecture which consists of many sized kernel which ensured better feature extraction from X-ray volumes. The possible explanation of erroneous results may have been because ground glass opacities (GGO) in those images were faint without consolidation. The proposed study thus provided a typical and successful solution for developing medical artificial intelligence system for screening and identification of Covid-19 disease. The work thus provided a high precision, non-invasive diagnostic system for screening and identification of Covid-19 disease using artificial intelligence and medical sciences.

VII. FUTURE WORK

There are still limitations and future work of this study, the major one being able to access and collect more data on other type of lung pneumonia which would further help improve its specificity. There may exist more suitable hyper-parameters for the proposed architecture which can help to classify the X-ray volumes with greater accuracy. More optimized version of CovAI-Net may be possible as a future work. Although there are many studies on prediction of Covid-19 using CT volumes [19], we are considering it as a future work to train CovAI-Net on CT volumes for prediction of lung diseases with greater accuracy.

REFERENCES

- [1] D. Shen, G. Wu, H. Suk. 2017 Deep learning in medical image analysis. *Annu. Rev. Biomed. Eng.* 19, 221–248. (doi:10.1146/annurev-bioeng-071516-044442)
- [2] M. Anthimopoulos, S. Christodoulidis, L. Ebner, et al. Lung Pattern Classification for Interstitial Lung Diseases Using a Deep Convolutional Neural Network. *IEEE Trans Med Imaging.* 2016;35(5):1207-1216. (doi:10.1109/TMI.2016.2535865)
- [3] J. Lei, J. Li, X. Li, et al. CT Imaging of the 2019 Novel Coronavirus (2019-nCoV) Pneumonia. *Radiology* 2020 Jan 31.
- [4] S. Albawi, T. A. Mohammed and S. Al-Zawi, "Understanding of a convolutional neural network," 2017 International Conference on Engineering and Technology (ICET), Antalya, 2017, page. 1-6.
- [5] N. Chen, M. Zhou, X. Dong, et al. Epidemiological and clinical characteristics of 99 cases of 2019 novel coronavirus pneumonia in Wuhan, China: a descriptive study [published January 29, 2020]. *Lancet.* (doi:10.1016/S0140-6736(20)30211-7)
- [6] S. Zhang, H. Li, S. Huang, et al. High-resolution CT features of 17 cases of corona virus disease 2019 in Sichuan province, China. *Eur Respir J* 2020. (doi: 10.1183/13993003.00334-2020)

- [7] H. Shi, X. Han, N. Jiang, et al. Radiological findings from 81 patients with COVID-19 pneumonia in Wuhan, China: a descriptive study. *Lancet Infect Dis.* 2020. ([https://doi.org/10.1016/S1473-3099\(20\)30086-4](https://doi.org/10.1016/S1473-3099(20)30086-4))
- [8] F. Chollet, "Keras", 2015 GitHub Repository, (<https://github.com/fchollet/keras>)
- [9] C. Szegedy, W. Liu, Y. Jia, et al., "Going deeper with convolutions," 2015 IEEE Conference on Computer Vision and Pattern Recognition (CVPR), Boston, MA, 2015, page. 1-9, (doi: 10.1109/CVPR.2015.7298594).
- [10] G. Huang, Z. Liu, L. V.D. Maaten, et al. "Densely Connected Convolutional Networks," 2017 IEEE Conference on Computer Vision and Pattern Recognition (CVPR), Honolulu, HI, 2017, page. 2261-2269.
- [11] F. Chollet, "Xception: Deep Learning with Depthwise Separable Convolutions," 2017 IEEE Conference on Computer Vision and Pattern Recognition (CVPR), Honolulu, HI, 2017, page. 1800-1807.
- [12] Kingma, P. Diederik, B. Jimmy. Adam: A Method for Stochastic Optimization. arXiv:1412.6980 [cs.LG], December 2014
- [13] C. Nwankpa, W. Ijomah, A. Gachagan, et al. Activation functions: Comparison of trends in practice and research for deep learning. arXiv 2018, arXiv:1811.03378.
- [14] S. Bustin, T. Nolan. Pitfalls of quantitative real-time reverse-transcription polymerase chain reaction. *J Biomol Tech.* 2004;15(3):155-166.
- [15] D. Ardila, A.P. Kiraly, S. Bharadwaj, et al. Author Correction: End-to-end lung cancer screening with three-dimensional deep learning on low-dose chest computed tomography. *Nat Med* 25, 1319 (2019). (<https://doi.org/10.1038/s41591-019-0536-x>)
- [16] K. Suzuki. Overview of deep learning in medical imaging. *Radiol Phys Technol.* 2017;10(3):257-273. (doi:10.1007/s12194-017-0406-5)
- [17] X. Wang., "A Weakly-supervised Framework for COVID-19 Classification and Lesion Localization from Chest CT," in *IEEE Transactions on Medical Imaging*, (doi: 10.1109/TMI.2020.2995965).
- [18] Z.-H. Zhou. A brief introduction to weakly supervised learning. *National Science Review*, 2017
- [19] J. Cheng, C. Weixiang, C. Yukun, et al. Artificial Intelligence Distinguishes COVID-19 from Community Acquired Pneumonia on Chest CT. *Radiology*, 2020. (<https://doi.org/10.1101/2020.03.20.20039834>)